

Ultracold atoms and Bose-Einstein condensates in optical lattices

Oliver Morsch and Ennio Arimondo

INFM, Dipartimento di Fisica, Università di Pisa, Via Buonarroti 2, I-56127 Pisa, Italy

Abstract. For ultracold and Bose-condensed atoms contained in periodic optical potential wells the quantized nature of their motion is clearly visible. The motion of the atomic wavepacket can also be accurately controlled. For those systems the long-range character of the atomic interaction and of the external potential play a key role in the quantum mechanical evolution. The basic facets of the experimental and theoretical research for atoms within optical lattice structures will be reviewed.

1 Introduction

Crystalline samples of cold atoms, now known as optical lattices, were initially investigated in the dissipative regime, as a tool to provide velocity damping, and hence a reduction of the kinetic energy of the atomic samples (for reviews see [1,2,3,4]). In fact the sub-Doppler cooling regime relies on the action of laser beams on the atomic motion in a standing wave configuration. The study of that regime also implied the possibility of trapping atoms in the sub-wavelength sized potential wells created by the laser beams. As soon it was clear that the standing wave patterns created by several intersecting laser beams provided by low-power diode lasers could be used to trap atoms in periodic structures, the field exploded. For instance a large experimental effort was made to probe directly the bound states of the atoms within the optical potential. After the initial experiments using one-dimensional (1D) lattices, several schemes were developed allowing an extension to two- and three-dimensions (2D and 3D). Very soon optical lattices were used as a flexible tool to modify the spatial periodicity of the cold atomic samples, and in some cases fancy spatial structures could be produced which the solid state physics community could only dream of. Moreover, important applications for atomic nanolithography have been realized.

Later, the research effort moved into the nondissipative, or conservative, regime, with the aim of reducing the scattering rate in the optical potential wells which ruled out coherent control over the wave-packet atomic motion. In fact, the interest in optical lattices shifted to using them as a test-bed for quantum mechanics. Such a shift in interest was enhanced when ultracold atomic samples represented by quantum degenerate gases were available for loading into the optical periodic potential. Bose-Einstein condensates (BEC's) represent flexible sources whose spatial dimensions and velocity spread can be controlled with large freedom, so that a condensate may be loaded with great accuracy into

the periodic potential created by intersecting laser beams. Thus the study of conservative optical lattices used to modify the spatial macroscopic wavefunction of BEC's has greatly expanded in the last few years.

In this work we will report on the most important aspects of the interaction between ultracold atoms, above and below the BEC temperature, within optical lattices. We will concentrate on those features more directly connected with the long-range interactions within the optical lattice. We will not, therefore, discuss some exciting investigations on the dynamical tunneling and chaotic behavior for atoms located within an optical periodic potential whose amplitude is periodically or randomly modulated [5,6]. Furthermore, we will not discuss the use of optical lattices in quantum computation schemes [7]. Moreover the subject of self generated periodic spatial structures will not be covered because separately treated in this book [8].

Section 2 will introduce the basic notions on the creation of optical lattices and the atomic response within the lattice, discussing first the near-resonant optical lattices that evolved from laser cooling schemes and then the non-dissipative, far-detuned optical lattices. Section 3 briefly reviews some of the experiments on ultracold atoms in optical lattices carried out since 1992, whilst section 4 deals with the more recent experiments in which Bose-Einstein condensates within optical lattices have been explored. The experimental results obtained by the Pisa group on Bloch oscillations, Landau-Zener tunneling and optical potential renormalization are there reported. Section 5 concludes the presentation.

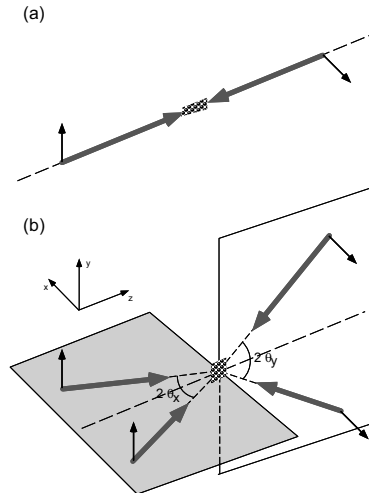


Fig. 1. Optical lattices in one and three dimensions. In both geometries, a frequency difference δ between the lattice beams can be used to create a moving or uniformly accelerated lattice.

2 Basic notions

2.1 Laser cooling

The simplest possibility to create a periodic potential for neutral atoms is to exploit the light-shift experienced by the atoms in a spatially modulated light field. In one dimension, this can be achieved by superposing two linearly polarized, counter-propagating laser beams with parallel or perpendicular polarizations (see Fig. 1(a)).

If the polarizations of the two laser beams are perpendicular to each other (see Fig. 2), an atom with two magnetic sub-levels in the ground state will see two interleaved standing waves of σ^+ and σ^- circularly polarized light. This so-called $lin \perp lin$ configuration was typical of the early experiments on optical lattices, as it provided both localization of the atoms at the troughs of the potential wells and a sub-Doppler cooling mechanism ("Sisyphus-cooling", in which atoms are preferentially pumped from a sub-level with locally high potential energy to the other sub-level with a potential minimum at that point, thus reducing the kinetic energy of the atoms as shown in Fig. 3.). For this combination of effects to work, the laser beams creating the optical lattice were detuned by a few natural linewidths from the atomic resonance (near-resonant optical lattices). In most configurations, the detuning was to the red side of the resonance, resulting in the atoms being trapped at the antinodes of the standing wave creating the lattice.

The 1D periodic structure created by two-counter-propagating laser beams can be generalized to two and three dimensions in different ways. Theodor Hänsch and his group in Munich used orthogonal pairs of beams whose relative phases were stabilized to create a constant lattice geometry [9]. A simpler approach was pioneered by Gilbert Grynberg's team at the ENS in Paris [10].

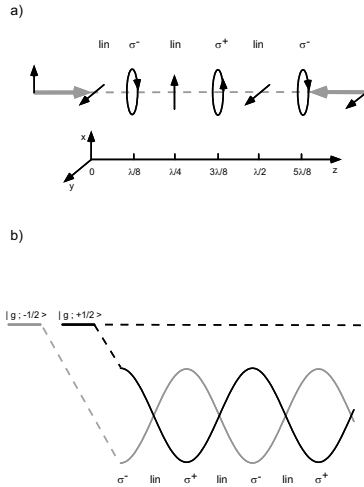


Fig. 2. A one-dimensional optical lattice in the $lin \perp lin$ configuration.

Figure 1(b) shows their beam geometry used to create a 3D lattice. In this setup, no active phase-control is necessary as a variation in phase of the beams will only lead to a spatial translation of the lattice without changing its intrinsic geometry. In 2D and 3D lattices, the arrangement of lattice wells can either be anti-ferromagnetic, with adjacent wells having orthogonal circular polarizations (as in the 1D example shown above), or ferromagnetic, in which case adjacent wells have the same circular polarization.

By changing the splitting angle θ between the two pairs of beams, the distance between neighbouring lattice wells in the ENS setup could be varied. This possibility has later also been used for experiments on BECs. In a 1D optical lattice with angle θ , the distance between neighboring wells (lattice constant) d can be varied through the angle θ between the two laser beams creating a lattice with

$$d = \frac{\pi \sin(\theta/2)}{k_L}, \quad (1)$$

where k_L is the laser wavenumber.

2.2 Conservative potential

After the exploration of the properties of near-resonant lattices, the research effort was concentrated on far-detuned lattices with detunings ranging from hundreds to thousands of linewidths, using both ultra-cold atoms and BECs. In these optical lattices the dissipative cooling mechanisms are not active and the optical lattice is described by a conservative potential. For a 1D lattice configuration as in Fig.1 with the two counterpropagating laser beams having the same polarization, the ac-Stark shift created by an off-resonant interaction between the electric field of the laser and the atomic dipole results a potential of the form

$$U(x) = U_0 \sin^2(\pi x/d), \quad (2)$$

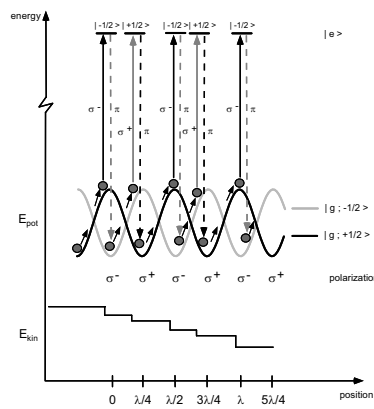


Fig. 3. The principle of Sisyphus cooling in a 1D optical lattice.

where U_0 is the depth of the potential and d the lattice constant. In a lattice configuration in which the two laser beams with wavevector k_L are counter-propagating, the usual choice of units are the recoil momentum $p_{rec} = \hbar k_L = Mv_{rec}$ and the recoil energy $E_{rec} = \hbar^2 k_L^2 / 2M$. In the case of an angle-geometry, it is more intuitive to base the natural units on the lattice spacing d and the projection $k = \pi/d$ of the laser wavevector k_L onto the lattice direction. However, the spatially periodic external potential leads naturally to a solid state physics approach. One can then define a Bloch momentum

$$p_B = \frac{2\hbar\pi}{d} = Mv_B, \quad (3)$$

corresponding to the full extent of the first Brillouin zone [11] or, alternatively, to the net momentum exchange in the lattice direction between the atoms and the two laser beams. In that frame of reference a possible choice for the energy unit is the Bloch energy defined as $E_B = \hbar^2(2\pi)^2 / Md^2$. These units can also be used for the case of the angle-geometry, making use of Eq. (1) for the connection between d and θ .

By introducing a frequency difference δ between the two beams, the lattice potential of Eq. (2) can be moved at a constant velocity v_{lat} given by

$$v_{lat} = d\delta \quad (4)$$

or accelerated with an acceleration a given by

$$a = d\frac{d\delta}{dt}. \quad (5)$$

3 Ultracold atoms

3.1 Early experiments: Local properties

The first experiments on optical lattices were aimed at local properties of the atoms trapped in the wells. Making a harmonic approximation to the potential at the centre of each well, it is straightforward to calculate the harmonic trapping frequency for a one-dimensional lattice as

$$\omega_{harm} = 2\frac{E_{rec}}{\hbar} \sqrt{\frac{U_0}{E_{rec}}}. \quad (6)$$

In a typical optical lattice experiment, atoms were first trapped and laser-cooled in a magneto-optical trap (MOT). After further cooling using optical molasses (essentially by switching off the magnetic fields of the MOT and increasing the detuning of the trap beams), the lattice laser beams were switched on. In order to demonstrate that the atoms were truly localized in the potential wells of the lattice, a series of experiments was carried out using pump-probe techniques [12]. By propagating a probe beam through the optical lattice that had a variable detuning from the lattice beams, Raman resonances could be

identified (see Fig. 4). These corresponded to an atom absorbing a photon from a lattice beam and emitting another into the probe beam (or vice versa) whilst changing its vibrational quantum number by unity. The measured positions of the Raman frequencies agreed with the calculated vibrational frequencies. These experiments were helped by the fact that due to Lamb-Dicke suppression of inelastic scattering, the Raman resonances were narrow enough to be individually resolvable.

Other experiments investigating the motion of the atoms in the lattice wells included the observation of breathing oscillations of the atomic wavepackets when then the well-depth was suddenly changed [13] as well as the collapse and revival of coherent wavepacket oscillations induced by rapidly shifting the lattice in space [14]. In both experiments, the wavepacket motion was inferred from the fluorescence light as the re-distribution of photons between the lattice beams due to the motion of the atoms led to intensity fluctuations that could be experimentally detected. Stimulated revivals were observed in 2000 by the lattice group in Hannover [15].

Information about coherence times of the atomic motion in optical lattices can also be obtained by creating coherent transients [16]. In this method, coherences between vibrational states are first created by a short probe pulse. Subsequently, during the lifetime of the coherence lattice photons will be preferentially scattered in the direction of the probe beam (now switched off). From the spectrum of these photons, vibrational frequencies and coherence times can be extracted [17].

3.2 Global properties

The nick-name "crystals bound by light" that was invented for optical lattices soon after their first experimental realization highlighted a property of these physical systems that was not visible in the early experiments, namely their periodic spatial structure. If optical lattices were, as predicted, "egg cartons" for atoms, then some direct evidence to that effect was desirable. An obvious experiment to carry out was Bragg-scattering of a probe beam off the planes of the "crystal", and in 1995 the groups in Munich and Gaithersburg [18,19] managed to do just that (see Fig. 5). They were able to show that when the

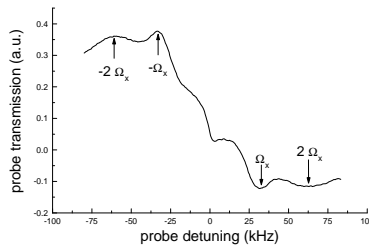


Fig. 4. Raman resonances in pump-probe spectroscopy along the x axis.

lattice beams were switched on, long-range spatial order was built up as the atoms were further cooled and localized in the periodically arranged potential wells of the lattice. When the lattice was switched off, the spatial order was lost on a time-scale consistent with the thermal motion of the atoms. By measuring the structure factor associated with the Bragg reflection, it was also possible to obtain information about the spatial localization of the atoms in the lattice wells [20].

Another global property of near-resonant optical lattices that was accessible to experimental verification was their response to external magnetic fields. Using an optical lattice with anti-ferromagnetic order of the atomic spins, the ENS group showed that by applying a magnetic field that differentially shifted the potential energies of the σ^+ and σ^- wells, a redistribution of population between the two sets of wells resulted in a macroscopic magnetization of the lattice [21]. The entire lattice, therefore, exhibited paramagnetic behaviour.

In near-resonant optical lattices, only a few percent of all the lattice sites actually contain an atom. Despite the consequent lack of atom-atom interactions, it was shown in 1996 that propagating excitations similar to sound waves can be created in optical lattices [22]. Through cycles of half-oscillations in the potential wells and subsequent optical pumping into the other magnetic sub-level of the ground state, propagating density modulations were created that could be detected via pump-probe spectroscopy. Moreover the first direct observation of Brillouin-like propagation modes in a dissipative periodic optical lattice was recently reported [23].

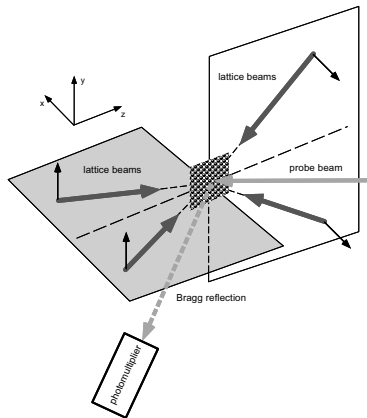


Fig. 5. Bragg scattering experiment on an optical lattice. From the Bragg-reflected probe beam, information about the spatial order and the localization of the atoms can be obtained.

3.3 Quasi-periodic lattices

Whilst so far we have stressed the regular, periodic structure of optical lattices, a number of interesting experiments have also been carried out in a quasi-periodic geometry. By adding an additional laser beam to the four-beam geometry described above, a quasi-periodic lattice structure can be created. The diffusion properties in such a lattice were studied by the group of Philippe Verkerk [24].

3.4 Far-detuned lattices

The fact that in a red-detuned, near resonant lattice the atoms are trapped at local maxima of the light intensity means that the coherent motion of the atomic wavepackets is frequently interrupted by spontaneous emission events. Early on in the development of optical lattices, schemes were developed that would provide trapping in locally "gray" or "dark" states in which the atoms absorb very few photons or no photons at all. These schemes were, appropriately, called "gray" or "dark" optical lattices [25].

In order to get rid completely of dissipative effects, it was, however, necessary to increase the detuning of the lattice beams from the atomic resonance and, at the same time, the beam intensity in order to keep a fixed lattice depth. As the spontaneous scattering rate decreases more rapidly with detuning than the light-shift or dipole force providing localization, in this manner optical lattices could be realized in which for the duration of the experiment (usually on the order of tens to hundreds of milliseconds) virtually no photons were scattered. The lack of photon scattering, on the other hand, also ruled out the Sisyphus cooling mechanism present in near-resonant lattices. In order further to cool atoms transferred into a far-resonant lattice, resolved-sideband Raman cooling was successfully employed by several groups [26,27,28]. As in trapped ion experiments, transitions towards lower vibrational levels were induced using a combination of laser beams and magnetic fields. In this way, a large fraction of the atoms could be cooled to the ground vibrational state of the lattice.

Another possibility to achieve the loading of atoms into the ground vibrational state (or, for shallow lattices, the ground state Bloch band) is to start from a Bose-condensed cloud of atoms, as will be discussed in the second part of this chapter.

3.5 A Lego-kit for quantum systems

Apart from the intrinsic interest in the characteristics of optical lattices, a number of experiments have used optical lattices as a tool for creating a specific quantum system whose properties could then be studied. Especially the precise experimental control of the lattice parameters (well depth, geometry) means that optical lattices can be used as a construction kit for quantum systems.

In a beautiful experiment [33,34], the group of Christophe Salomon at the ENS in Paris demonstrated Bloch oscillations of atomic matter waves delocalized over many lattice sites of a shallow optical lattice by accelerating the lattice and

measuring the resulting velocity of the atoms. Related experiments by Mark Raizen's team in Austin investigated Landau-Zener tunneling and Wannier-Stark ladders [29]. In an extension to this work, they were able to experimentally verify the non-exponential nature of the initial decay of a quantum system [30] and the associated Zeno and anti-Zeno effects exhibited by such systems when they are subject to frequent observations [31].

In a near-resonant lattice, Gilbert Grynberg's group at the ENS was able to create an asymmetric optical lattice with a ratchet-like potential that converted the random thermal motion of the atoms into directed motion [32].

4 Bose-condensed atoms

While in most of the original optical lattice experiments the atomic clouds had temperatures in the the micro-Kelvin range, corresponding to a few recoil energies of the atoms, atomic samples with sub-recoil energies are now routinely produced in Bose-Einstein condensation experiments. Since the first experimental realizations in 1995, many aspects of Bose-Einstein condensed atomic clouds (BECs) have been studied [39], ranging from collective excitations to superfluid properties and quantized vortices. The properties of BECs in periodic potentials constitute a vast new field of research initially explored in [40,41]. Several experiments have made use of the periodic optical potential produced by a pulsed standing wave to manipulate the condensate or to explore its properties [42,43,44,45,46,47,48,49]. In the following, we will concentrate on studies of the condensate within the periodic optical lattice. The first step in that direction was taken by the investigation of the tunneling of BECs out of the one-dimensional potential wells of a shallow optical lattice in the presence of gravity [50]. More recently the phase properties of the condensate wavefunction occupying the whole optical lattice have involved such intriguing concepts as number squeezing [51] and the Mott insulator transition [52]. The tunneling of the condensate between neighboring wells, controlled by varying the optical lattice potential depth, determine the overall properties of the macroscopic wavefunction. Thus the condensate response within a 1D optical lattice can be described as an array of tunneling junctions, as pointed out in [50] and later explored in [53,54] in connection with the superfluid properties of the condensate wavefunction. Coherent acceleration of BECs adiabatically loaded into optical lattices was demonstrated in [55,56], with Bloch oscillations observed for small values of the lattice depth, while a Landau-Zener breakdown occurred when the lattice depth was further reduced and/or the acceleration increased. The expansion of the condensate array was explored initially in [57] and later in [58]. The high level coherent control over this artificial solid state system was demonstrated in [59], where the BEC was carefully loaded into the lattice ground state by adiabatically turning on the optical lattice. The different dependence of the condensate population on the temperature for the 1D optical lattice was pointed out by ref. [60].

Most experiments were based on the production of the condensate through the standard technique, followed by an adiabatic load into the optical lattice.

Often the magnetic trap was switched off when the optical lattice was switched on. However, a larger condensate density is realized when the interaction between the condensate and the lattice takes place inside the magnetic trap, and both of them are subsequently switched off to allow time-of-flight imaging. The Florence group [53] has developed a different approach by producing the condensate directly inside the optical lattice which is adiabatically loaded during the evaporating cooling stage. The main advantage of this approach is that the phase coherence of the condensate over the whole optical lattice structure is built up during the condensate formation process. The main disadvantage is that the optical lattice is on during the whole evaporation process, and the spontaneous losses produced by the optical lattice should be heavily reduced by further increasing the detuning of the optical lattice lasers. While a large majority of the experiments have loaded the condensate into 1D optical lattices, experiments on 2D lattices were performed by Greiner *et al.* [61], and the Mott-Hubbard transition of ref. [52] was realized in a 3D optical lattice.

If the momentum spread of the atoms loaded into an optical lattice structure is small compared to the characteristic lattice momentum p_B , then their thermal de Broglie wavelength will be large compared to the lattice spacing d and will, therefore, extend over many lattice sites. A description in terms of a coherent delocalized wavepacket within a periodic structure is then appropriate and leads us directly to the Bloch formalism first developed in condensed matter physics. In the tight-binding limit ($U_0 \gg 10 E_{\text{rec}}$), the condensate in the lattice can be approximated by wavepackets localized at the individual lattice sites (Wannier states). This description is more intuitive than the Bloch picture in the case of experiments in which the condensate is released from a (deep) optical lattice into which it has previously been loaded adiabatically.

4.1 BEC theory in optical lattices

In Bose-Einstein condensates, interactions between the constituent atoms are responsible for the non-linear behavior of the BEC and can lead to interesting phenomena such as solitons [62] and four-wave mixing with matter waves [63]. As the atoms are extremely cold, collisions between them can be treated by considering only s -wave scattering, which is described by the scattering length a_s . Modeling the interatomic interaction as hard-core collisions, one can simplify the treatment using a mean-field description which leads to the famous Gross-Pitaevskii equation [64], the validity of which has been demonstrated in numerous experiments. For a BEC in an optical lattice, one expects an effect due to the mean-field interaction similar to the one responsible for determining the shape of a condensate in the Thomas-Fermi limit: The interplay between the confining potential and the density-dependent mean-field energy leads to a modified ground state that reflects the strength of the mean-field interaction. Applied to a BEC in a periodic potential, one expects the density modulation imposed on the condensate by the potential (higher density in potential troughs, lower density where the potential energy is high) to be modified in the presence of mean-field interactions. In particular, the tendency of the periodic potential

to create a locally higher density where the potential energy of the lattice is low will be counteracted by the (repulsive) interaction energy that rises as the local density increases.

The description of a condensate in a 1D array of coupled potentials wells is based on the total Hamiltonian

$$H_{tot} = \frac{-\hbar^2}{2M} \nabla^2 + U_0 \sin^2(\pi \frac{x}{d}) + g |\Psi(\mathbf{r})|^2, \quad (7)$$

with the interaction parameter g given by

$$g = \frac{4\pi\hbar^2 a_s}{M}, \quad (8)$$

and $\Psi(\mathbf{r})$ the condensate wavefunction at position \mathbf{r} .

As the interaction term is expected to distort the band structure of the condensate in the lattice [40], it should affect all measurable quantities (Rabi frequency, amplitude of Bloch oscillations, and tunneling probability). In Ref. [65], the authors derived an analytical expression in the perturbative limit (assuming $U_0 \ll E_B$) for the effect of the mean-field interaction on the ground state of the condensate in the lattice. Starting from the Gross-Pitaevskii equation for the condensate wavefunction in a one-dimensional optical lattice (*i.e.* a one dimensional Hamiltonian equivalent to that of Eq. (7)), they found that the effect of the mean-field interaction could be approximately accounted for by substituting the potential depth U_0 with an effective potential

$$U_{eff} = \frac{U_0}{1 + 4C}, \quad (9)$$

with the dimensionless parameter C given by [65]

$$C = \frac{\pi n_0 a_s}{k_L^2 \sin^2(\theta/2)} = \frac{n_0 g}{E_B}, \quad (10)$$

corresponding to the ratio of the nonlinear interaction term and the Bloch energy. The C parameter contains the peak condensate density n_0 , the scattering length a_s , and the atomic mass M . From the dependence of C on the lattice angle θ it follows that a small angle θ (meaning a large lattice constant d) should result in a large interaction term C . The reduction of the effective potential given by Eq. (9) agrees with the intuitive picture of the back-action on the periodic potential of the density modulation of the condensate imposed on it by the lattice potential. For repulsive interactions, this results in the effective potential being lowered with respect to the actual optical potential created by the lattice beams.

4.2 Theoretical advances

The properties of Bose-Einstein condensates within optical lattices have been examined in a large number of theoretical papers, predicting a variety of phenomena, often making use of the strict analogies with cases previously studied

within the context of solid state physics and nonlinear dynamics. We will list here the principal research lines that have characterized this research so far.

The collective excitations of the condensate within optical lattices, and their probe, have been determined [66,67,68], and those analyses have stimulated the experimental investigations in refs. [47,48,49]. A strong deformation of the Bloch energy bands of the condensate produced by the nonlinear atomic interactions has been predicted in refs. [69,70,71]. Different mechanisms of breaking down the Bloch oscillation, all of them connected to the interatomic interactions, have been discussed in refs. [72,73,74,75].

The thermal and quantum decoherence for an array of multiple condensates within an optical lattice, introduced in refs. [76,77], are an important issue requiring more detailed studies, both theoretically and experimentally. The Bose-Hubbard-Hamiltonian for atoms in an optical lattice, introduced by Jaksch *et al.* [41], was analyzed in ref. [78] through a mean-field approximation generalization of the Bogoliubov approach; later it was applied to determine the conditions for the number squeezing in that transition [79].

A number of papers have pointed out the existence of additional solutions for the evolution of the condensates within optical lattices: instabilities, solitons (shape preserving excitations), breathers (excitations characterized by internal oscillations), and self-trapping states or intrinsic localized modes (wavepacket localized around few lattice sites) [74,80,81,82]. Those predictions have often made use of theoretical analogies with other nonlinear classical and quantum problems, involving the sine-Gordon equation, the discrete nonlinear Schrödinger equation and other nonlinear physics problems. Spatial instabilities of the condensate within the optical lattice, with a spontaneous breaking in the spatial periodicity, have been predicted by Wu and Niu [75].

4.3 Experimental results

Bloch oscillations For 1D optical lattice, a linear increase of the detuning δ between the two laser beams forming the lattice provides to the optical lattice the constant acceleration given by Eq. (5). As the lattice can only transfer momentum to the condensate in units of $2\hbar k$, the acceleration of the condensate leads to higher momentum classes as the acceleration time increases. With an initial momentum spread of the condensate much less than the Bloch momentum p_B and since the adiabatic switching transfers the momentum spread into lattice quasimomentum, the different momentum classes $p = \pm np_B$ (where $n = 0, 1, 2, \dots$) occupied by the condensate wavefunction can be resolved directly after the time-of-flight. In the experiments of refs. [55,56] with the optical lattice in the horizontal direction and the atomic wave diffraction monitored in the time-of-flight detection, the accelerated momentum classes showed up as diffraction peaks in the time-of flight absorption images as in Fig.6. Up to $6 p_B$ momentum could be transferred to the condensate preserving the phase-space density of the condensate during the acceleration, a result indicating that no heating or reduction of the condensate fraction occurred. Measuring the average velocity of the condensate from the occupations of the different momentum states, the

Bloch oscillations of the condensate velocity corresponding to a Bloch-period $\tau_B = h/(Ma_s d)$ could be detected. Note in Fig.6 that while the Bloch oscillation takes place, the condensate wavefunction coherently occupies two neighboring velocity classes. In a configuration with the optical lattice oriented along the vertical direction [50,56], the different momentum classes emitted from the condensate travel in space separately because of the acceleration due to gravity. Thus the condensate absorption images after the time of flight show one or two atom laser pulses corresponding to the single or double momentum class occupied by the condensate at the time of the release.

Landau-Zener tunneling At large acceleration of the lattice or at a decreased lattice depth, not all of the condensate could be coherently accelerated up to the final velocity of the lattice. Such condensate loss can be interpreted in terms of Landau-Zener tunneling of the condensate out of the lowest band when the edge of the Brillouin zone is reached. Each time the condensate is accelerated across this edge, the fraction undergoing tunneling into the first excited band is given by the Landau-Zener probability P_{LZ} [33,55,59]:

$$P_{LZ} = e^{-a_c/a} \quad (11)$$

with the critical acceleration a_c given by

$$a_c = \frac{\pi U_0^2}{16\hbar^2 k}. \quad (12)$$

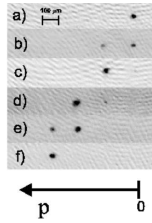


Fig. 6. Coherent acceleration of a Bose-Einstein condensate. In (a)-(f) $U_0 = 2.3 E_{\text{rec}}$ $a = 9.81 \text{ m s}^{-2}$, the condensate being accelerated for 0.1, 0.6, 1.1, 2.1, 3.0 and 3.9 ms, respectively. The separations between the different spots vary because the detection occurred after different time delays.

Such tunneling produces the following mean velocity v_m of the condensate at the end of the acceleration process for a final velocity v_B of the lattice:

$$v_m = (1 - P_{LZ})v_B. \quad (13)$$

In ref. [55] it was verified that this formula correctly described the tunneling of the condensate at low values of the condensate density by varying both the potential depth and the lattice acceleration. In the configuration with the optical lattice oriented along the vertical direction [50,56], the different momentum classes emitted from the condensate travel in space separately because of the acceleration due to gravity. Thus the condensate absorption images after the time of flight (Fig.7) showed a part of the population confined in the optical lattice, and several laser pulses corresponding to the different momentum class occupied by the condensate.

Optical potential renormalization In order to measure accurately the variation of the effective potential U_{eff} with the interaction parameter C as given by Eq. (9), the Landau-Zener tunneling out of the lowest Bloch band for small lattice depth was studied in a regime where the parameter C modified the optical potential experienced by the condensate [55,56]. Therefore, the variation of the final mean velocity v_m was studied as a function of the condensate density. The density was varied by changing the mean harmonic frequency of the magnetic trap. From the mean velocity the effective potential was then calculated using the Landau-Zener probability given above, with the critical acceleration determined by the effective potential

$$a_c = \frac{\pi U_{\text{eff}}^2}{16\hbar^2 k}. \quad (14)$$

Fig. 8 shows the ratio U_{eff}/U_0 as a function of the parameter C for the experimental investigation in two different geometries of the optical lattice, counter-propagating and in an angle-geometry with $\theta = 29$ deg. As predicted by Eq. (10), the reduction of the effective potential is much larger in the angle geometry. The theoretical predictions of Eq. (9) given by the theory of [65] are also shown in the figure. An effective potential may also be derived within the framework of a tight-binding approximation using Wannier states, i.e. describing the condensate within each potential minimum potential through the solution of the Gross-Pitaevskii equation while neglecting the overlap with neighboring potential minima [83], a very weak tunneling of the condensate preserving the overall phase relation of the condensate wavefunction. The tight-binding predictions presented in Fig. 8 provide a better agreement with experimental results than those of Eq.(9).

Squeezed states and Mott insulator Because the condensate is a superfluid, described by a wavefunction exhibiting long-range phase coherence, if the lattice potential is turned on smoothly, the condensate remains in the superfluid phase.

In this regime a delocalized condensate wavefunction minimizes the total energy of the many-body system, the phase of the atomic wavefunction being well determined, with a fluctuating atom number at each lattice site. This applies as long as the atom-atom interactions are small compared to the tunnel coupling. Instead, when the repulsive atom-atom interactions are large compared to the tunnel coupling, the total energy is minimized when each site of the optical lattice is filled with the same number of atoms. Approaching this Mott-insulator quantum phase transition, with the lattice site number commensurate to the atom number, the wavefunction phase coherence is lost. Meanwhile, the fluctuations in the number of atoms per site are reduced and finally go to zero. In addition, in the superfluid regime the excitation spectrum is gapless, whereas the Mott insulator phase exhibits a gap in the excitation spectrum.

The first important step in modifying a condensate from a coherent state to a Fock state was taken by Orzel *et al.* [51] who realized squeezed states in a 1D optical lattice. By properly choosing the depth of the optical potential and the amplitude of the mean field interaction term in Eq. (7), the authors were able to reach a regime where deviation from the coherent state wavefunction for the condensate became significant. An increase in the phase fluctuations of the condensate wavefunction was measured in the interference of atom waves released from the optical lattice. From this, a squeezing in the number of atoms occupying the lattice sites was derived by assuming a minimum uncertainty state.

The experimental realization of the Mott insulator in a 3D optical lattice in ref. [52] required a cubic optical lattice where a volume with 65 sites in each single direction was occupied, with potential depth around $U_0 = 12 E_{\text{rec}}$. Adiabatic loading of a condensate of 2×10^5 atoms into such a lattice produced a state whose coherence properties were tested as usual by the interference pattern following a time-of-flight. At a potential depth larger than $10 E_{\text{rec}}$ the interference pattern presented an incoherent background, gaining more strength increasing the potential depth until that background was the only visible feature in the interference. That loss of interference was a first sign of the Mott-insulator regime, with a Fock state without macroscopic phase coherence characterizing the occupation of the single wells. Evidence of the phase transition was gained by monitoring the quick restoration of the phase coherence, quick as compared to the restoration produced by the inhomogeneous dephasing of the superfluid condensate wavefunction under the application of a magnetic energy gradient. Additional strong evidence was provided by the direct measurements of the gap in the excitation spectrum of the Mott insulator, in contrast to the superfluid phase where the excitation spectrum is gapless.

5 Conclusion and Outlook

We have provided a brief overview of the research work performed on cold atomic samples (laser cooled or evaporatively cooled to the quantum degenerate regime) located within the periodic potential created by an optical interaction, concen-

trating our attention on the phenomena where the long range order of the external potential is imprinted onto the atomic wavefunction. As far as quantum degenerate gases within optical lattices are concerned, recently the field has greatly flourished with new experimental groups joining the crowded space and theory groups proposing new exciting schemes and pointing out the occurrence of interesting phenomena. It seems that Bose-Einstein condensates in optical lattices could be the test-bed for a large variety of theoretical models. It is obvious that this flourishing of ideas and of measurements will continue still for some time, because additional configurations could be explored, the control on the atoms and the optical lattices will progress, and finally because other phenomena may occur when Fermi degenerate gases will be loaded in optical lattices. The detailed comparison between theory and experiments dealing with Bose-Einstein condensates within optical lattices requires heavy numerical solutions of the 3D Gross-Pitaevskii equation. However, the recent realization of nearly 1D Bose-Einstein condensates could simplify the theoretical analysis.

But even with non-condensed, ultra-cold gases the versatility of optical lattices in realizing and studying quantum systems will certainly provide interesting challenges to physicists in the future. Studies of cold collisions and diffusion properties in optical lattices are but two of the areas in which a lot of work still needs to be done. Moreover, experiments will test the schemes in which the coherent motion of the atoms in far-detuned optical lattices could be exploited to realize quantum logic gates.

Acknowledgments

The collaboration of D. Ciampini, M. Cristiani and J.H. Müller to the experimental results reported in the present work is gratefully acknowledged. This work was supported by the MURST through the PRIN2000 Initiative, by the INFN through the Progetto di Ricerca Avanzata ‘Photon matter’, and by the EU through the Cold Quantum Gases Network, Contract No. HPRN-CT-2000-00125. O.M. gratefully acknowledges a Marie Curie Fellowship from the EU within the IHP Programme.

References

1. P.S. Jessen and I.H. Deutsch, *Adv. At. Mol. Opt. Phys.* **37**, 95 (1996).
2. G. Grynberg and C. Triché, in *Coherent and Collective Interactions of Particles and Radiation Beams* edited by A. Aspect, W. Barletta, and R. Bonifacio (IOS Press, Amsterdam) (1996).
3. D.R. Meacher, *Cont. Phys.* **39**, 329 (1998).
4. G. Grynberg and C. Robilliard, *Phys. Rep.* **355**, 335 (2001).
5. D.A. Steck, W.H. Oskay and M.G. Raizen, *Science* **293**, 274 (2001) and references therein.
6. W.K. Hensinger, H. Häffner, A. Browaeys, N.R. Heckenberg, K. Helmerson, C. McKenzie, G.J. Milburn, W.D. Phillips, S.L. Rolston, H. Rubinstein-Dunlop, and B. Upcroft, *Nature* **412**, 52 (2001) and references therein.

7. See, e.g., I.H. Deutsch and P.S. Jessen, Phys. Rev. A **57**, 1972 (1998), and D. Jaksch, H.-J. Briegel, J.I. Cirac, C.W. Gardiner, and P. Zoller, Phys. Rev. Lett. **82**, 1975 (1998).
8. G. Kurizki, S. Giovanazzi, D. O'Dell, A. I. Artemiev *New Regimes in Cold Gases Via Laser-Induced Long-Range Interactions*, in “Dynamics and Thermodynamics of Systems with Long Range Interactions”, T. Dauxois, S. Ruffo, E. Arimondo, M. Wilkens Eds., Lecture Notes in Physics Vol. 602, Springer (2002), (in this volume)
9. A. Hemmerich and T.W. Hänsch, Phys. Rev. Lett. **70**, 410 (1993).
10. G. Grynberg, B. Lounis, P. Verkerk, J.Y. Courtois, and C. Salomon, Phys. Rev. Lett. **70**, 2249 (1993).
11. see, e.g., C. Kittel, *Introduction to Solid State Physics* (Wiley, New York, 1996).
12. P. Verkerk, B. Lounis, C. Salomon, C. Cohen-Tannoudji, J.Y. Courtois, and G. Grynberg, Phys. Rev. Lett. **68**, 3861 (1992).
13. P. Rudy, R. Eijnisman, and N.P. Bigelow, Phys. Rev. Lett. **78**, 4906 (1997).
14. G. Raithel, W.D. Phillips, and S.L. Rolston, Phys. Rev. Lett. **81**, 3615 (1998).
15. F.B.J. Buchkremer, R. Bumke, H. Levsen, G. Birkl, and W. Ertmer, Phys. Rev. Lett. **85**, 3121 (2000).
16. C. Triché, L. Guidoni, P. Verkerk, and G. Grynberg, in *OSA TOPS on ultra-cold atoms and BEC*, edited by K. Burnett, vol. 7, p. 82, (OSA, Washington D.C., 1996).
17. O. Morsch, P.H. Jones, and D.R. Meacher, Phys. Rev. A **61**, 023410 (2000).
18. M. Weidemüller, A. Hemmerich, A. Görlitz, T. Esslinger, and T.W. Hänsch, Phys. Rev. Lett. **75**, 4583 (1995).
19. G. Birkl, M. Gatzke, I.H. Deutsch, S.L. Rolston, and W.D. Phillips, Phys. Rev. Lett. **75**, 2823 (1995).
20. A. Görlitz, M. Weidemüller, T.W. Hänsch, and A. Hemmerich, Phys. Rev. Lett. **78**, 2096 (1997).
21. D.R. Meacher, S. Guibal, C. Mennerat, J.Y. Courtois, K.I. Petsas, and G. Grynberg, Phys. Rev. Lett. **74**, 1958 (1995).
22. J.Y. Courtois, S. Guibal, D.R. Meacher, P. Verkerk, and G. Grynberg, Phys. Rev. Lett. **77**, 40 (1996).
23. L. Sanchez-Palencia, F.-R. Carminati, M. Schiavoni, F. Renzoni, and G. Grynberg, Phys. Rev. Lett. **88**, 133903 (2002).
24. L. Guidoni, B. Dépret, A. di Stefano, and P. Verkerk, Phys. Rev. A **60**, R4233 (1999).
25. A. Hemmerich, M. Weidemüller, T. Esslinger, C. Zimmermann, and T.W. Hänsch, Phys. Rev. Lett. **75**, 37 (1995).
26. S.E. Hamann, D.L. Haycock, G. Klose, P.H. Pax, I.H. Deutsch, and P.S. Jessen, Phys. Rev. Lett. **80**, 4149 (1998).
27. H. Perrin, A. Kuhn, I. Bouchoule, and C. Salomon, Europhys. Lett. **42**, 395 (1998).
28. V. Vuletic, C. Chin, A.J. Kerman, and S. Chu, Phys. Rev. Lett. **81**, 5768 (1998).
29. K.W. Madison, M.C. Fischer, and M.G. Raizen, Phys. Rev. A **60**, R1767 (1999).
30. S.R. Wilkinson, C.F. Bharucha, M.C. Fischer, K.W. Madison, P.R. Morrow, Qian Niu, B. Sundaram, and M.G. Raizen, Nature **387**, 575 (1997).
31. M.C. Fischer, B. Guttierrez-Medina, and M.G. Raizen, Phys. Rev. Lett. **87**, 040402 (2001).
32. C. Mennerat-Robilliard, D. Lucas, S. Guibal, J. Tabosa, C. Jurczak, J.Y. Courtois, and G. Grynberg, Phys. Rev. Lett. **82**, 851 (1999).
33. M. Ben-Dahan, E. Peik, J. Reichel, Y. Castin, and C. Salomon, Phys. Rev. Lett. **76**, 4508 (1996);
34. E. Peik, M. Ben Dahan, I. Bouchoule, Y. Castin, and C. Salomon, Phys. Rev. A **55**, 2989 (1997).

35. S.R. Wilkinson, C.F. Bharucha, K.W. Madison, Qian Niu, and M.G. Raizen, *Phys. Rev. Lett.* **76**, 4512 (1996).
36. Qian Niu, Xian-Geng Zhao, G.A. Georgakis, and M.G. Raizen, *Phys. Rev. Lett.* **76**, 4504 (1996).
37. M. Raizen, C. Salomon, and Qian Niu, *Phys. Today* **50** (7), 30 (1997).
38. C.F. Bharucha, K.W. Madison, P.R. Morrow, S.R. Wilkinson, B. Sundaram, and M.G. Raizen, *Phys. Rev. A* **55**, R857 (1997).
39. See reviews by W. Ketterle, D.S. Durfee and D.M. Stamper-Kurn, and by E. Cornell *et al.* in *Bose-Einstein condensation in atomic gases*, edited by M. Inguscio, S. Stringari and C. Wieman (IOS Press, Amsterdam) (1999).
40. K. Berg-Sørensen and K. Mølmer, *Phys. Rev. A* **58**, 1480 (1998).
41. D. Jaksch, C. Bruder, J.I. Cirac, C.W. Gardiner, and P. Zoller, *Phys. Rev. Lett.* **81**, 3108 (1998).
42. M. Kozuma, L. Deng, E.W. Hagley, J. Wen, R. Lutwak, K. Helmerson, S.L. Rolston, and W.D. Phillips, *Phys. Rev. Lett.* **82**, 871 (1999).
43. Yu.B. Ovchinnikov, J.H. Müller, M.R. Doery, E.J.D. Vredenburg, K. Helmerson, S.L. Rolston, and W.D. Phillips, *Phys. Rev. Lett.* **83**, 284 (1999).
44. E.W. Hagley, L. Deng, M. Kozuma, M. Trippenbach, Y. B. Band, M. Edwards, M. Doery, P. S. Julienne, K. Helmerson, S. L. Rolston, and W. D. Phillips, *Phys. Rev. Lett.* **83**, 3112 (1999).
45. J. Stenger, S. Inouye, A. P. Chikkatur, D. M. Stamper-Kurn, D. E. Pritchard, and W. Ketterle, *Phys. Rev. Lett.* **82**, 4569 (1999); and erratum: *Phys. Rev. Lett.* **84**, 2283 (2000).
46. J.E. Simsarian, J. Denschlag, M. Edwards, C.W. Clark, L. Deng, E.W. Hagley, K. Helmerson, S.L. Rolston, and W.D. Phillips, *Phys. Rev. Lett.* **85**, 2040 (2000).
47. J. M. Vogels, K. Xu, C. Raman, J. R. Abo-Shaeer, and W. Ketterle, *Phys. Rev. Lett.* **88**, 060402 (2002)
48. J. Steinhauer, R. Ozeri, N. Katz, and N. Davidson, *Phys. Rev. Lett.* **88**, 120407 (2002).
49. R. Ozeri, J. Steinhauer, N. Katz, and N. Davidson, *Phys. Rev. Lett.* **88**, 220401 (2002).
50. B.P. Anderson and M. Kasevich, *Science* **282**, 1686 (1998).
51. C. Orzel, A.K. Tuchman, M.L. Fenselau, M. Yasuda, and M.A. Kasevich, *Science* **291**, 2386 (2001).
52. M. Greiner, O. Mandel, T. Esslinger, T.W. Hänsch, and I. Bloch, *Nature* **415**, 6867 (2002).
53. S. Burger, F. Cataliotti, C. Fort, F. Minardi, M. Inguscio, M.L. Chiofalo, and M.P. Tosi, *Phys. Rev. Lett.* **86**, 4447 (2001).
54. F.S. Cataliotti, S. Burger, C. Fort, P. Maddaloni, F. Minardi, A. Trombettoni, A. Smerzi, and M. Inguscio, *Science* **293**, 843 (2001).
55. O. Morsch, J.H. Müller, M. Cristiani, D. Ciampini, and E. Arimondo, *Phys. Rev. Lett.* **87**, 140402 (2001).
56. M. Cristiani, O. Morsch, J. H. Müller, D. Ciampini, and E. Arimondo, *Phys. Rev. A* **65**, 063612 (2002).
57. P. Pedri, L. Pitaevskii, S. Stringari, C. Fort, S. Burger, F.S. Cataliotti, P. Maddaloni, F. Minardi, and M. Inguscio, *Phys. Rev. Lett.* **87**, 220401 (2001).
58. O. Morsch, M. Cristiani, J.H. Müller, D. Ciampini, and E. Arimondo, cond-mat 0204528.
59. J. Hecker-Denschlag, J. E. Simsarian, H. Häffner, C. McKenzie, A. Browaeys, D. Cho, K. Helmerson, S. L. Rolston, and W. D. Phillips, *J. Phys. B: At. Mol. Opt. Phys* in press (2002).

60. S. Burger, F. S. Cataliotti, C. Fort, P. Maddaloni, F. Minardi and M. Inguscio, *Europhys. Lett.* **57** 1 (2002).
61. M. Greiner, I. Bloch, O. Mandel, T.W. Hänsch, and T. Esslinger, *Phys. Rev. Lett.* **87**, 160405 (2001).
62. S. Burger, K. Bongs, S. Dettmer, W. Ertmer, K. Sengstock, A. Sanpera, G.V. Shlyapnikov, and M. Lewenstein, *Phys. Rev. Lett.* **83**, 5198 (1999).
63. L. Deng, E.W. Hagley, J. Wen, M. Trippenbach, Y. Band, P.S. Julienne, J.E. Sim-sarian, K. Helmerson, S.L. Rolston, and W.D. Phillips, *Nature* **398**, 6724 (1999).
64. F. Dalfovo, S. Giorgini, L.P. Pitaevskii, and S. Stringari, *Rev. Mod. Phys.* **71**, 463 (1999).
65. D.I. Choi and Qian Niu, *Phys. Rev. Lett.* **82**, 2022 (1999).
66. A. Brunello, F. Dalfovo, L. Pitaevskii, and S. Stringari, *Phys. Rev. Lett.* **85**, 4422 (2000).
67. M.L. Chiofalo, S. Succi, and M.P. Tosi, *Phys. Rev. A* **63**, 063613 (2001).
68. M.Krämer, L. Pitaevskii, and S. Stringari, *Phys. Rev. Lett.* **88**, 180404 (2002).
69. J.C. Bronski, L.D. Carr, B. Deconink, and J.N. Kutz, *Phys. Rev. Lett.* **86**, 1402 (2001).
70. B. Wu, R.B. Diener, and Qian Niu, *Phys. Rev. A* **65**, 025601 (2002).
71. D.Diakonov, L.M. Jensen, C.J. Pethick, and H. Smith, e-print: cond-mat/0111303.
72. B. Wu and Qian Niu, *Phys. Rev. A* **61**, 023401 (2000).
73. O.Zobay and B.M. Garraway, *Phys. Rev.* **61** 033603 (2000).
74. A. Trombettoni and A. Smerzi, *Phys. Rev. Lett.* **86**, 2353 (2001).
75. B. Wu and Qian Niu, *Phys. Rev. A* **64**, 061603 (2001).
76. L. Pitaevskii, and S. Stringari, *Phys. Rev. Lett.* **88**, 180402 (2001).
77. A. Cuccoli, A. Fubini, V. Tognetti, and R. Vaia, *Phys. Rev. A* **64**, 061601 (2001).
78. D. van Oosten, P. van der Straten, and H.T.C. Stoof, *Phys. Rev. A* **63** 053601 (2001).
79. K.Burnett, M. Edwards, C.W. Clark, and M. Shotton, *J. Phys. B: At. Mol. Opt. Phys.* **35**, 1671 (2002).
80. F. Kh. Abdullaev, B. B. Baizakov, S. A. Darmanyan, V. V. Konotop, and M. Salerno, *Phys. Rev. A* **64**, 043606 (2001).
81. V.V. Konotop and M.Salerno, *Phys. Rev. A* **65**, 021602(R) (2002).
82. N. Tuskada, *Phys. Rev. A* **65**, 063608 (2002).
83. M. Kalinski, G. Metakis, and W.P. Schleich, private communication.

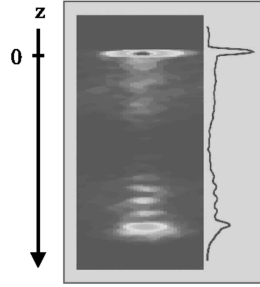


Fig. 7. Time-of-flight image and, on the left, transverse vertical profile for the Landau-Zener tunnelling of a condensate from a 1-D optical lattice oriented vertically. The $p = +|n|p_B$ atomic momentum classes are separated by the gravity, pointing downwards. The large condensate amplitude near $z = 0$ corresponds to the population confined in the lattice. The atomic momentum classes generate the atom laser pulses detected after a 10.1 ms time of flight, with $U_0 = 10 E_{\text{rec}}$ and condensate acceleration for 10 ms.

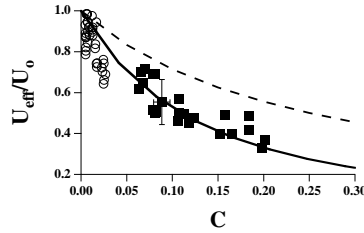


Fig. 8. Dependence on the C parameter for the effective potential U_{eff} , normalized to the applied optical potential U_0 , for the two lattice geometries of ref. [55]. The experimental results for the counter-propagating geometry (open circles) and angle geometry with $\theta = 29$ deg (filled squares) are plotted together with the theoretical prediction of ref. [65](dashed line) and of ref. [83](continuous line). Parameters in these experiments were $a = 23.4 \text{ m s}^{-2}$ and $U_0 = 2.2 E_{\text{rec}}$ for the counter-propagating lattice and $a = 3.23 \text{ m s}^{-2}$ and $U_0 = 5.7 E_{\text{rec}}$ for the angle geometry.